

# A S T

## Antarctic Submillimetre-wave Telescope



### Submillimetre Astronomy Working Group

Authors: Vincent Minier (CEA Saclay), Luca Olmi (INAF Arcetri), Emanuele Daddi (CEA Saclay), Gilles Durand (CEA Saclay), Frank Israel (Leiden), Carsten Kramer (IRAM & Cologne), Marco de Petris (INFN Rome), Lucia Sabbatini (La Sapienza, Rome), Nicola Schneider (CEA), Luigi Spinoglio (INAF Rome), Pascal Tremblin (CEA), Nick Tothill (Exeter), Luca Valenziano (INAF Bologna).

Advisers: Frank Helmich (FIRI), IPEV, PNRA, Pierre-Olivier Lagage (CEA Saclay), Nicola Epchtein (ARENA), Paolo Saraceno (INAF Rome), John Storey (UNSW), Slimane Bensammar (Observatoire de Paris).

Industrial partners: EIE and Thales Alenia Space.



Working document

Version 1.0 - CMC Working Meeting

# Table of contents

CHAPTER 1: SCIENCE CASES .....	4
1 SUBMILLIMETRE ASTRONOMY: SCIENCE AND CONTEXT .....	4
1.1 Astronomy in the submillimetre/far-infrared .....	4
1.2 Telescope facilities: present and forthcoming .....	4
1.3 Why evaluating potential science with a FIR/submm telescope at Dome C ? .....	4
2 SUBMILLIMETER OBSERVATIONS OF GALACTIC STAR FORMATION .....	5
2.1 Galactic star formation .....	5
2.2 The formation of high-mass stars .....	6
2.3 Example of science cases .....	6
2.4 Extension of telescope capabilities to the mid-infrared .....	7
3 SPECTRAL LINES AND THE INTERSTELLAR MEDIUM .....	7
3.1 The dense, warm gas traced by CO, HCN, HCO+ .....	8
3.2 Phase-structure of the ISM and the NII 205- $\mu$ m line .....	9
3.3 Prestellar cores and deuterated species .....	9
4 MAGELLANIC CLOUD .....	10
4.1 Dust: a major ISM component .....	10
4.2 The Magellanic Clouds: ideal astrophysical laboratories .....	10
4.3 A proposed FIR/Submm observing program .....	11
5 GALAXY EVOLUTION .....	12
5.1 Galaxy Formation and Evolution, the case for a large telescope operating in the FIR .....	12
5.1.1 The need for sensitive FIR observations to map the buildup of stars and black holes .....	12
5.1.2 Required depths .....	13
5.2 Synergies and complementarity to Herschel and ALMA .....	14
5.3 SCUBA2 and related surveys .....	14
5.4 A case for a much larger facility ? .....	14
5.5 Accessing the best studied fields .....	15
6 FAR-INFRARED AND SUBMILLIMETER SPECTROSCOPY OF GALAXIES ALONG THEIR EVOLUTION .....	16

7	A POTENTIAL CASE FOR DOME C: THE SUNYAEV-ZEL'DOVICH EFFECT.....	18
7.1	<b>Introduction.....</b>	<b>18</b>
7.2	<b>Peculiarities for Dome C SZE observations.....</b>	<b>20</b>
8	UNIQUE SCIENCE CASE: UNDERSTANDING SUN CORONAL MASS EJECTION .....	22
8.1	<b>Impact.....</b>	<b>22</b>
8.2	<b>Other facilities.....</b>	<b>23</b>
8.3	<b>Observations and requirements .....</b>	<b>23</b>
	CHAPTER 2: SITE TESTING .....	25
9	PWV FROM ATMOSPHERIC TRANSMISSION MEASUREMENTS .....	25
10	THERMAL GRADIENT AND VARIABILITIES UP TO 46 M HIGH .....	26
11	FROST FORMATION.....	28
	CHAPTER 3: TELESCOPE FACILITY .....	31
	(IN PARTNERSHIP WITH EIE AND THALES ALENIA SPACE) .....	31
12	TOP-LEVEL REQUIREMENTS.....	31
12.1	<b>Active Surface .....</b>	<b>31</b>
12.2	<b>Optical Design .....</b>	<b>31</b>
12.3	<b>Pointing and Tracking.....</b>	<b>31</b>
13	EXTENSION TO MID-INFRARED .....	32

Working document - version 1.0 - CMC-WG meeting

# CHAPTER 1: SCIENCE CASES

## 1 Submillimetre astronomy: science and context

### 1.1 Astronomy in the submillimetre/far-infrared

Far-infrared/submillimetre (FIR/submm - 100 to 1000  $\mu\text{m}$ ) astronomy is the prime technique to study the 'cold Universe' and unveil the birth and early evolution of planets, stars and galaxies. It is a relatively new branch of astronomy at the frontier between IR and radio astronomy. FIR/submm continuum observations are particularly powerful to measure the luminosities, temperatures and masses of cold dust emitting objects because dust enshrouded star-forming regions emit the bulk of their energy between 60 and 500  $\mu\text{m}$ . The submm/FIR range of the spectrum or THz regime is also rich in several lines that are the only means to study the kinematical structure of the interstellar medium (ISM) of galaxies. They allow to probe different physical regimes, i.e. regions of widely different densities and temperatures, depending on their excitation levels and critical abundances. Observations at these wavelengths with a large telescope will primarily lead to breakthroughs in the study of star formation at all scales and understand its cosmic history back to the early Universe as well as in the understanding of galaxy evolution. Asteroids, Debris disks, Planet formation, Dust origin in evolved stars, Interstellar dust and Polarisation of dust in the Universe are also potential science drivers for FIR/submm astronomy.

### 1.2 Telescope facilities: present and forthcoming

What is the context today of submm astronomy ? Two major submm facilities will become available in the coming years: the Herschel Space Observatory, a FIR/submm (60-500  $\mu\text{m}$ ) telescope in Space and ALMA, a ground-based mm-wave (350  $\mu\text{m}$ -7 mm) interferometer on the Chajnantor plateau in the northern Atacama desert. Both facilities will have their specific niches. Herschel will have the ability to carry out large area imaging surveys of both the distant Universe and the nearby interstellar medium in our own Galaxy. ALMA will make possible ultra deep searches for primordial galaxies (Blain 2001), as well as detailed kinematical investigations of individual protostars. However, both Herschel and ALMA will have their own limitations. The Herschel telescope (3.5 m) will suffer from its only moderate angular resolution, implying a fairly high extragalactic confusion limit and preventing the study of individual protostars in all but the nearest star-forming clusters of our Galaxy. ALMA will suffer from a small field of view (10") and limited observable conditions in the FIR/submm, making extensive wide-field mapping impossible given the amount of time necessary to cover large star-forming complexes and fields of primordial galaxies. Beside these two major facilities, there is a constellation of submm/FIR telescope projects in operation or in study, aboard balloons (e.g. BLAST, OLIMPO, PILOTE etc), aboard an airplane (SOFIA), aboard satellites (e.g. Akari; SPICA) and on high-altitude plateaux and mountains (e.g. APEX; CCAT, a 25-m telescope project)

### 1.3 Why evaluating potential science with a FIR/submm telescope at Dome C ?

Beside Herschel and ALMA, there is thus a clear need for a large (>10m) single-dish telescope: **(1)** operating at 200-450  $\mu\text{m}$  and providing **(2)** better angular resolution than Herschel and **(3)** wider-field mapping capabilities than ALMA, making large-scale mapping with a relatively good angular resolution ( $\sim 1''$ ) possible and well matched with thermal infrared space telescope (e.g. Spitzer). New sites are therefore intensively tested because the 200-350-450- $\mu\text{m}$  windows at Chajnantor open less than 30% of wintertime at an observable level, probably less than 10% at 200  $\mu\text{m}$ . The stability of the atmosphere is an equally important parameter when comparing the sites and Dome C may stand out as being far more stable than Chilean sites. Equipped with FIR/submm imagers and spectrometers, a European telescope at Dome C in Antarctica might be able to operate in all atmospheric windows between 200  $\mu\text{m}$  and 1 mm, and very regularly at 350 and 450  $\mu\text{m}$  all year. Dome C could become the European observatory in Antarctica.

## 2 Submillimeter observations of galactic star formation

### 2.1 Galactic star formation

Dust is the most robust tracer to study the cycling of material from dying stars to the ionized, atomic, and molecular phases of the interstellar medium (ISM), into star forming cloud cores. Atoms, ions, and molecules are subject to complex chemical processing, depletions onto grains, and excitation conditions, whereas dust is stable in most phases of the ISM. Most of the Star Formation (SF) activity in the ISM takes place in cold, dense cores, which represent a very early stage of the SF process before collapse results in the formation of a central protostar. Because of their temperature ( $\ll 20$  K), these *pre-stellar* cores are best observed in the dust continuum at submm wavelengths and through molecular line emission. Dust is optically thin in the Far-Infrared (FIR) to (sub)mm over most of the Galaxy, so that its emission and absorption simply depend on emissivity, column density and temperature.

Several (sub)mm to FIR Galactic surveys are currently being carried out, and after *Herschel* and SCUBA-2 on JCMT will become operational, Galactic Plane (GP) surveys will identify pretty much all the Star Forming Regions (SFRs) in the Galaxy, in the form of dense dust cores. At the pre- and proto-cluster level (0.1-0.2 pc) we will be pretty much complete to a mass sensitivity of  $\sim$  few up to  $10s M_{\odot}$  and with Spectral Energy Density (SEDs; see e.g. Fig.1.1) in the range  $\sim 70 - 850$  micron. Therefore, the low mass end of the distribution of cloud core masses will still be limited by sensitivity in surveys of nearby clouds, and also the high mass end will remain uncertain because the massive clouds are very rare and hence distant and difficult to find without large, devoted surveys.

Thus, much of the subsequent work in the field will be devoted to form a complete census of the mass distribution of cloud cores down to masses that can form brown dwarf stars, and to the characterization of the evolutionary phase and physical parameters of these cores, which will allow to discriminate among different SF scenarios. These observations will require high spatial resolution and sensitivity, as well as frequency agility, which can all be delivered by a large single-dish operating at submm wavelengths.

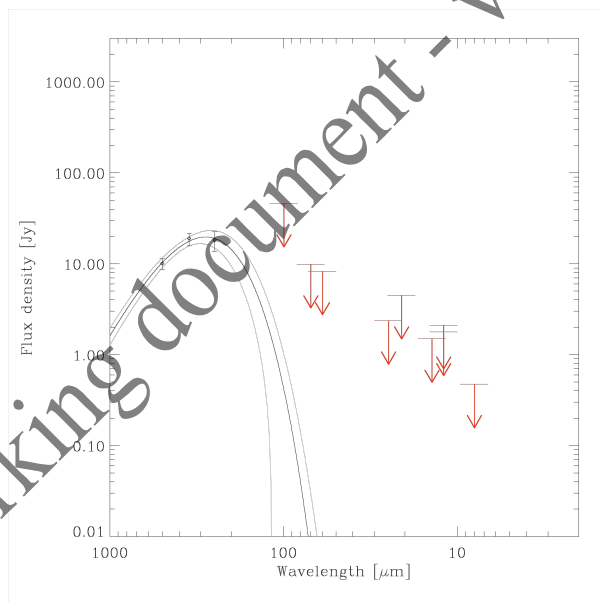


**Figure 2.1** The SED of the coldest BLAST source in the Vulpecula region (V11,  $T=10$  K). The FIR spectrum turns over in the BLAST bands (from Chapin et al. 2008).

The properties of star-forming cores depend strongly on the physical processes leading to their formation. In addition, a comparison of the mass distribution of the pre-stellar cores (the core mass

function, CMF) with the stellar initial mass function (IMF) may reveal what process is responsible for determining stellar masses.

While surveys with BLAST and *Herschel* are sensitive enough to determine the large-scale physical parameters of the dense cores in the nearest SFRs, it is doubtful that they will have the required angular resolution to determine the cores' mass and temperature internal distribution, even in the nearest clouds, due to confusion in crowded fields. It is important to note that the only way to reach unambiguous conclusions on the core structure and mechanical balance, thus setting constraints on the theoretical models describing the initial conditions for individual protostellar collapse, is to reconstruct the temperature and column-density profiles simultaneously through multi-band imaging (at wavelengths longward of  $\sim 200 \mu\text{m}$ ). Ground observations are invaluable to achieve the required angular resolution.

## 2.2 The formation of high-mass stars

The formation of high-mass stars (HMS,  $M \gg 8 M_{\odot}$ ) poses even more specific questions about the process of SF. Like low-mass stars (LMS), HMS form in dense cores within molecular cloud complexes. Unlike LMS, however, a massive central protostar is formed while still deeply embedded and accreting its final mass. Thus, at this stage the copious UV flux emitted by the central massive star creates a HII region which is expected to slow down and halt the accretion of cloud material (e.g., Stahler et al. 2000), thus preventing the formation of a more massive star. This is clearly a specific theoretical problem, and to solve it a few competing families of models have been proposed.

Observationally, once young massive stars have developed an ultracompact HII (UCHII) region, they can be easily detected in the IR and radio centimeter continuum. However, *earlier* stages of massive SF, i.e. pre-stellar, are also best detected via FIR or (sub)mm dust continuum as shown by the BLAST project (Chapin et al. 2008). Since the earliest phases of high-mass star formation have been studied in very few objects up to now, the initial conditions of this process remain poorly known. Also very schematic remains our knowledge of what are the characteristics of molecular cloud complexes in terms of temperature, density, and velocity structure, as well as non-thermal support and degree of fragmentation, that may affect the process of HMSF.

This is causing the slightly larger granularity in the CCAT maps, where each point is sampled for less time. Appropriate observing conditions have been assumed at each site, i. e., drier conditions for shorter wavelengths; an elevation of  $60^{\circ}$  and the same amount of mapping time have been assumed for both telescopes.

It is important to note that the only way to reach unambiguous conclusions on the core structure, thus setting constraints on the theoretical models describing the initial conditions for individual protostellar collapse, is to reconstruct the temperature and column-density profiles simultaneously through multi-band imaging (at wavelengths longward of  $\sim 200 \mu\text{m}$ ). Ground observations are invaluable to achieve the required angular resolution. Another important potential issue in cluster-forming regions, that

We can clearly see the effects of angular resolution. At 200 micron, the two nearby cores are clearly separated in the CCAT simulated map, and are barely resolved in the ASO map (ASO – Antarctic Submillimeter Observatory, an ALMA-like 12m antenna). However, at 350 micron, ASO is no longer able to separate the two cores, which are seen as a single object instead. The advantage of the larger CCAT diameter is quite evident in this specific example. However, the noise in the maps, expressed as MJy/srad, are quite similar due to the larger ASO beam, and the mapping speed is higher with ASO.

## 2.3 Example of science cases

First example:

- Immediate objective in the submm

The IMF is largely determined by the Core Mass Function (CMF), thus it is fundamental to understand the physical processes leading to the formation of pre-stellar cores. One needs:

- Accurate bolometric luminosities
- Temperature and density profiles
- Multi-wavelengths observations
- CMF down to sub-solar masses
- Telescope requested
  - Feasible with 12m for nearest clouds, but the angular resolution would require an aperture  $>\sim 25\text{m}$  for HMSFRs and brown dwarfs
- Instrument requested
  - If bolometer: at least  $2\times 2$  arcmin<sup>2</sup>
  - If heterodyne: deuterated species at THz frequencies
- Sensitivity requested
  - $\sim$  few mJy/beam
- Overall time needed to achieve the science program:  $\sim 10\text{s}$  to  $100\text{s}$  hrs

Second example:

- Immediate objective in the submm

*Follow the physical and chemical evolution of gas/dust content of massive star forming cores and envelopes during their evolution. A combination of chemistry, excitation and kinematics is required.*

- Will require molecular line surveys in the 500-2000 GHz range
- Telescope requested
  - 25m
- Instrument requested
  - Heterodyne/bolometer arrays
- Sensitivity requested
  -
- Overall time needed to achieve the science program:  $\sim 100\text{s}$  hrs

Other immediate science goals would be: (i) Measure the star formation rate and history Galaxy-wide. (ii) Determine the upper mass end of the IMF, measure SFRs, efficiency, triggers, evolution/time scale of early phases of massive stars. (iii) Obtain the complete inventory of cold dust in the Galactic Plane. (iv) Establishing the existence and nature of star formation thresholds as a function of ISM properties across a full range of galactocentric radii, metallicity and environmental conditions. (v) Determining the relative importance of global vs. local mechanisms that give rise to star formation. (vi) Provide templates, recipes and prescriptions for extra-gal science.

#### 2.4 Extension of telescope capabilities to the mid-infrared

If the telescope could be used simultaneously at both submm and MIR wavelengths it would convert this instrument in a powerful SED-machine, thus able to immediately discriminate between pre- and proto-stellar cores. In fact, while for extremely cold cores multi-wavelengths observations in the submm may be enough to constrain the peak of the SED and thus the core temperature (see Fig.1), for warmer cores observations at MIR wavelengths are required to constrain the SED. This ability would also allow to determine whether MIR emission is truly associated with a given core, or rather is emitted by a nearby, more evolved core. This is currently achieved using archive data from, e.g., MSX and *Spitzer*. However, the MSX data are often not sensitive enough and the MIPS observations at 70 micron are limited in dynamic range; both suffers from limited angular resolutions.

### 3 Spectral lines and the interstellar medium

The combination of submm studies with molecular line observations of dense gas tracers is a powerful method for determining the physical and kinematical parameters of SFRs. A 12m telescope at Dome C will open the realm of submillimeter observations at high angular and spectral resolutions from

Antarctica. The excellent atmospheric transmission from Dome A will allow routine observations in the 450 and 350  $\mu\text{m}$  atmospheric windows. Under exceptionally good conditions, the THz windows between 300 and 200  $\mu\text{m}$  become accessible. Dome C will allow for routine spectroscopic observations of several key species of the ISM.

Existing frequency surveys of e.g. the Orion KL star formation region in the submillimeter windows show a plethora of species and the great potential of a 12m telescope at Dome C for studying the chemistry of the ISM. Important tracers of the dense, warm molecular gas tracing the immediate neighbourhood of star formation, are the high-rotational lines of CO, HCN, HCO<sup>+</sup>. Among the most important spectral lines, is the NII line at 205  $\mu\text{m}$  line which will allow to study the distribution and kinematics of the ionized gas. Studying the ground-state rotational transitions of deuterated H<sub>3</sub><sup>+</sup> will significantly improve our understanding of the chemical network in the ISM, and in particular in dense, molecular cloud cores, the future sites of star formation.

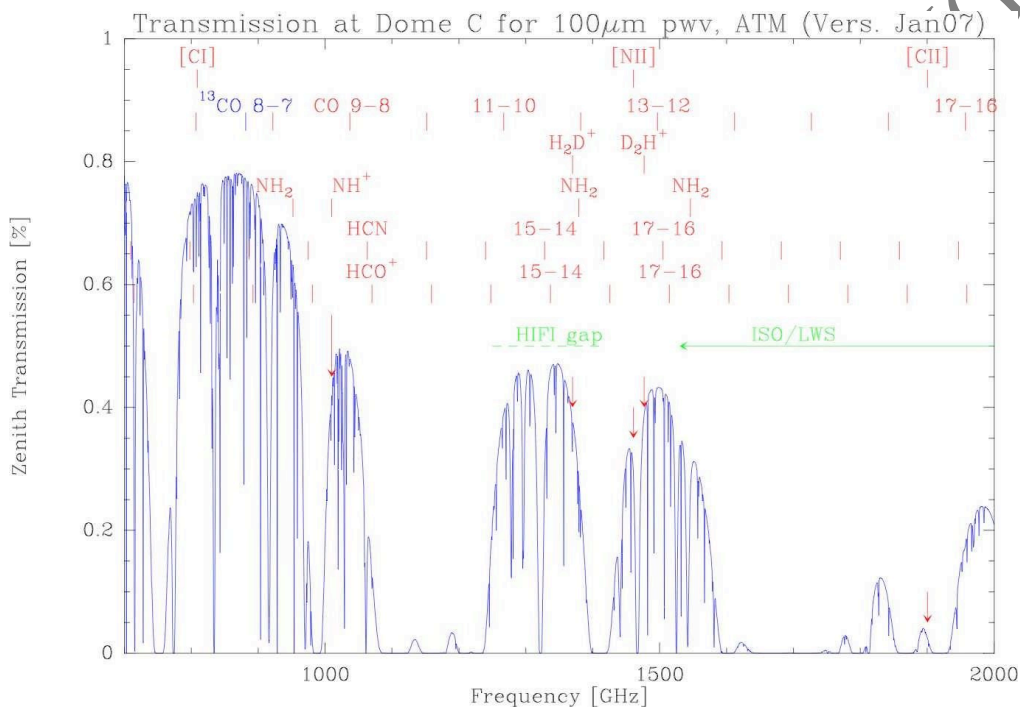


**Figure 3.1** Atmospheric transmission and a few key spectral lines of the ISM between 700 GHz and 2 THz. The atmospheric windows centered near 350  $\mu\text{m}$  (860 GHz), 290  $\mu\text{m}$  (1050 GHz), 230  $\mu\text{m}$  (1300 GHz), and 200  $\mu\text{m}$  (1500 GHz) are clearly visible. The transmission curve was calculated using ATM (J. Pardo) for Dome C altitude assuming excellent atmospheric conditions, i.e. 100  $\mu\text{m}$  precipitable water vapour (pwv) (cf. the FTS spectrum obtained at 93  $\mu\text{m}$  pwv at Cerro Sairecabur by Marrone et al. 2005).

### 3.1 The dense, warm gas traced by CO, HCN, HCO<sup>+</sup>

High rotational transitions of CO, HCN, HCO<sup>+</sup> allow to trace the density and temperature structure of the warm and dense gas found in the immediate neighbourhood of active star formation sites, e.g. hot cores and photon dominated regions.

The rotational ladder of the chemically very stable molecule CO allows to trace a wide range of excitation conditions depending on the rotational transition  $J$ : the upper energy level is 2.8 J (J+1) Kelvin and the critical density is  $4 \times 10^3 J^3/\text{cm}^3$ . The CO 13--12 transition lying in the 200  $\mu\text{m}$  window for example is only excited in warm and dense gas, as it has an upper energy level of 510 K and a critical density of  $10^7 \text{cm}^{-3}$ . While KAO and ISO observed integrated intensities of high- $J$ , i.e. THz, CO lines with resolutions of about an arcminute, only few velocity resolved observations of these lines exist to date. The optically thin <sup>13</sup>CO(8-7) line at 880 GHz is also accessible from the ground, providing the



rare opportunity to obtain direct measures of the column densities of the warm and dense gas (e.g. Kramer et al. 2004, Wyrowski et al. 2006 using the KOSMA 3m and the APEX 12m telescopes).

Due to their large dipole moments, THz transitions of HCN and HCO<sup>+</sup> trace very high densities and excitation conditions. The Orion KL frequency survey in the 350- $\mu$ m window by Comito et al. (2005) using the CSO shows very strong HCN and HCO<sup>+</sup> lines of between 30 and 100 K main beam temperatures.

### 3.2 Phase-structure of the ISM and the NII 205- $\mu$ m line

Heterodyne observations of the bright, but so-far largely unexplored NII 205- $\mu$ m line allows to study the distribution and kinematics of the warm, low-density ionized gas and is hence an excellent, extinction free probe of star formation. The relative importance of the various ISM phases will be disentangled by comparing NII, CII(158  $\mu$ m), HI, CO line profiles tracing the ionized, atomic, and molecular medium.

The NII 205- $\mu$ m line has nearly the same critical density as the CII 158- $\mu$ m line for electron impact excitation. NII is an excellent, extinction free tracer of star formation. In contrast to the radio continuum, which is emitted by thermal and non-thermal processes, which are difficult to separate, NII emission is not polluted by non-thermal radiation. The critical densities are 44 cm<sup>-3</sup> for the 205- $\mu$ m line and 293 cm<sup>-3</sup> for the 122- $\mu$ m line, for an electron temperature of 8000 K. However, N<sup>+</sup> takes 14.5 eV to form, so that (unlike C<sup>+</sup>) it is only found in ionized gas regions. Therefore, the line ratio in ionized media is essentially only a function of the N<sup>+</sup>/C<sup>+</sup> abundance ratio - which is not sensitive to the hardness of the stellar radiation fields since it takes about the same energy to form N<sup>++</sup> as it does to form C<sup>++</sup>.

Oberst et al. (2006) have used this technique to deduce that 27% of the observed CII emission from the Carina Nebula arises from the diffuse ionized gas (the rest arising from photon dominated regions (PDRs)). The 122- $\mu$ m NII line has been used in a similar fashion (Kramer et al. 2005, Contursi et al. 2002) to show that up to 30% of the CII observed with ISO/LWS in the spiral arms of M83 and M51 stem from the ionized phase. However, studies with the 122- $\mu$ m line, are compromised by the density dependence of the NII 122  $\mu$ m CII ratio - an effect greatly mitigated by using the 205- $\mu$ m NII line. Supplementing FIR lines tracing the high density ionized gas are e.g. the OIII lines at 88 and 52  $\mu$ m.

### 3.3 Prestellar cores and deuterated species

H<sup>3+</sup> is a key species in the chemical network at play in the ISM. However, it is observationally accessible only via infrared absorption spectroscopy. In prestellar cores, H<sup>3+</sup> is one of the very few molecules expected to stay in the gas-phase, when almost all C,N,O bearing molecular species have frozen-out on dust grains.

Spectroscopic observations of the isotopomers of H<sup>3+</sup> should therefore in principle allow to trace the kinematics in the inner, cold, dense pre-stellar cores, before the onset of star formation. Very high deuteration levels have been observed in pre-stellar cores, allowing to use H<sub>2</sub>D<sup>+</sup> and D<sub>2</sub>H<sup>+</sup> to study their physical conditions (Walmsley et al. 2004, Flower et al. 2004). Note that D<sup>3+</sup> lacks any dipole moment, similar to H<sup>3+</sup>, and can thus only be detected via absorption studies in the NIR.

The ortho- H<sub>2</sub>D<sup>+</sup> ground-state transition at 372 GHz has been detected in dark clouds, but also towards low-mass protostars and in proto-planetary disks (Stark et al. 1999, 2004, Vastel et al. 2004, Harju et al. 2006, Ceccarelli et al. 2004). However, the ground-state transition of para- H<sub>2</sub>D<sup>+</sup> at 1370 GHz has not been detected yet despite several attempts (Philips et al. 1985, Boreiko & Betz 1993). It is noteworthy that this transition was lying outside the ISO/LWS wavelength range and will also lie outside the HIFI/Herschel tuning range. The situation is similar for D<sub>2</sub>H<sup>+</sup>. The para-D<sub>2</sub>H<sup>+</sup> ground-state line at 692 GHz has been detected by Vastel et al. (2004) in the core of 16293E, the ortho- D<sub>2</sub>H<sup>+</sup> line at 1477 GHz has not been detected yet.

## 4 Magellanic cloud

### 4.1 Dust: a major ISM component

Dust particles are an important component of the interstellar medium. They shield fragile molecules such as CO from destruction by UV photons, and they allow other molecules such as H<sub>2</sub> to form by grain-surface reactions. Dust grain populations are the outcome of local conditions, such as metallicity and energetics. For instance, shocks from expanding SNRs are a major and efficient source of dust particle erosion and destruction on short timescales (Jones et al. 1994, 1996). This rapid erosion may be countered by efficient accretion of dust particles in quiescent, dense (molecular) gas clouds. Several authors have attempted to extract the resulting equilibrium particle size distribution from measurements of Solar-Neighbourhood objects (e.g. Mathis et al 1977). At the small end of their distribution, hot very small grains excited by the absorption of a single photon (Draine & Anderson, 1985) and even smaller PAHs (Léger & Puget 1984) occur. Including these additional populations, Weingartner & Draine (2001) constructed metallicity-dependent size distributions for carbonaceous and silicate grains pertinent to the different conditions in the Galaxy, the LMC and the SMC and other physically-based dust emission models are also becoming available (e.g. Li & Draine 2001; Zubko et al. 2003).

As the erosion timescales are short compared to accretion timescales, variations in ambient conditions may rapidly and substantially alter local grain size distributions. Alteration of the balance between big grains and very small grains may cause noticeable changes in SED shapes. This appears to be the case in the strong starburst environment characterizing the dwarf galaxy NGC 1569 (Lisenfeld et al. 2002). A small but clear emission excess at submillimeter wavelengths is unlikely to be caused by cold 'classical' big grains. Rather, most of the submillimeter and far-infrared emission from this galaxy appears to originate in very small grains with a relatively small total mass. Thus, in environments with extensive dust grain processing, traditional interpretations easily overestimate dust masses, and consequently underestimate both gas-to-dust ratios and gas masses deduced from dust emission.

Even if this interpretation were not correct, models still need to take into account some form of very cold dust, particularly in regions of low metallicity. For instance, 'very cold' dust emission has also been found in NGC 4631 (Dumke et al. 2004), in Virgo blue compact dwarf galaxies (Popescu et al. 2002) and in the MW itself (Reach et al. 1995). Other explanations invoke fractal dust aggregates or diffuse non ionizing UV radiation. The difficulty in interpreting the local 'very cold' emission is our lack of absolute submm measurements within the MW, and the difficulty in extragalactic studies is the lack of spatial resolution and hence wide range of temperatures within the beam.

As a major part of the astration cycle, the ISM plays an essential role in galaxy evolution. It is thus important to gain insight in the processes that govern dust grain processing and dust particle size distributions. Studying far-infrared/submillimeter SEDs as a function of varying ambient conditions is a very promising way of making significant progress.

### 4.2 The Magellanic Clouds: ideal astrophysical laboratories.

The closest Milky Way satellites, the Large Magellanic Cloud (LMC) and the Small Magellanic Cloud (SMC) provide the ideal astrophysical laboratories for such investigations. With distances of 50 kpc (Feast 1999) and 61 kpc (Keller & Wood 2006) respectively, they are ten times closer than other major systems in the Local Group of galaxies, and typically 40-100 times closer than other 'nearby' galaxies. Their external nature but close proximity simultaneously provides full global and unimpeded very detailed views. They allow us to resolve parsec-sized structures, making it possible to study ISM processes unambiguously on scales dominated by a single star. They have low dust and metal abundances, different from each other and from the Milky Way, thus providing three different metallicity baselines.

The LMC, with a metallicity one quarter solar (Dufour et al. 1984), has a mass of  $9 \times 10^9 M_{\odot}$  (van der Marel et al. 2002), a size of about 8 kpc and a star formation rate of  $0.1 M_{\odot}/\text{yr}$  (Whitney et al. 2007).

The SMC, with a metallicity one tenth solar (Dufour et al. 1984) has a mass of  $2.5 \times 10^9 M_{\odot}$ , a size of about 3 kpc, and a star formation rate of  $0.05 M_{\odot}/\text{yr}$  (Wilke et al. 2003). Metallicities show little variation across either system, but luminous star formation has created a very large range of ambient radiation field intensities in each Cloud. UV radiation field intensities in both Clouds range from less than those in the MW Solar Neighbourhood to hundreds of times higher.

We can therefore study the effects of ambient radiation fields at constant metallicities. Because of their particular nature, the Magellanic Clouds provide well-determined environments representing a variety of metallicities and energy densities in which the resulting properties of the interstellar medium can be studied in a detailed and systematic manner not offered elsewhere. Not only is by far the largest part of the Milky Way (MW) inaccessible to such studies, but all ISM studies in the MW also greatly suffer from confusion caused by line-of-sight crowding and distance ambiguities. In the LMC and the SMC, everything is essentially at the same distance, and determinations of mass and luminosity are unambiguous and directly comparable. The LMC is particularly favourable because its limited depth and its viewing angle of  $35^{\circ}$  (van der Marel & Cioni 2001) place only a single cloud along any line of sight.

### 4.3 A proposed FIR/Submm observing program

At present, no systematic far-infrared/submillimeter survey of either LMC or SMC exists. Shortwards of 200 microns, IRAS and Spitzer maps are available, not allowing, however, to investigate the crucial submillimeter excess. This may become possible, for the first time, if the Herschel Space Observatory mission is successful. One of its accepted Open Time Key Programmes aims at conducting uniform surveys of the LMC and the SMC in the 250, 350 and 500 micron bands.

Here, we propose to conduct similar surveys of both Clouds in the 200, 350, and 450 micron bands with a 12 m telescope at the best possible site on Earth, providing an order of magnitude more collecting area and more importantly, 3.5 times higher linear resolution. Such resolutions will render the survey sensitive to interstellar conditions on scales of 1-2 parsec, i.e. allows us to distinguish the spheres of influence of individual stars - a feat not possible with the Herschel surveys, even if they are fully successful. We propose a baseline observing program involving 2300 hours of integration time per band (total observing time can therefore be reduced considerably by simultaneous observation), per Cloud. We have assumed NEFDs of 750 mJy/beam, 150 mJy/beam, and 150 mJy/beam at 20 microns, 350 microns, and 450 microns respectively. For the LMC ( $8^{\circ} \times 8^{\circ}$ ) this yields sensitivities of 138 MJy/sr, 7.5 MJy/sr and 3.5 MJy/sr, or 45 mJy/beam, 5 mJy/beam, and 4 mJy/beam. For the SMC, the same integration time yields sensitivities 4 times better (because the surface area to be covered is 16 times less than for the LMC). With these numbers, the proposed survey will not only have a significantly better resolution than the expected Herschel maps, but for the LMC also a better sensitivity per (smaller!) beam than Herschel at 350 and 500 microns, and for the SMC even much better sensitivity.

The resulting images will provide unique insight in the conditions dominating dust in the interstellar medium of galaxies. As the measurements cover the Rayleigh-Jeans side of the warm dust emission spectrum, they are relatively little affected by large temperature-related uncertainties, and allow study of the coldest ISM dust. The dust maps will show the distribution of (cool) dust on typical scales of 1-2 parsecs corresponding to typical gas column densities of  $10^{21}$  and  $10^{22}$  H-atoms/cm<sup>2</sup> for the LMC and SMC, respectively. The measurements are similar to those planned for the Herschel SPIRE experiment, but their 3.5 times higher linear resolution (12 times higher area resolution) render them fully complementary to these, and in fact uniquely provide the extremely high linear resolution that is needed to study the effects of stars on their immediately surrounding ISM. The high resolution also will allow even better identification of embedded young stellar objects (YSOs), as they will now have an order of magnitude higher contrast with their surroundings than in the Herschel maps. The variation in dust properties gleaned from the dust maps together with the inventory of radiation sources and gas densities obtained from other already existing datasets will allow us, in particular, to study changes in interstellar grain excitation and size distribution, i.e. follow in detail the process of

dust particle erosion in areas dominated by radiation, by shocks, and at significantly different metallicities.

An alternative approach may also be considered, if the Herschel observations are successful. Instead of duplicating uniform surveys, the resulting maps may be used to select emission regions for deeper integration. Depending on the scope of such a program, the dust emission in both LMC and SMC may then be probed an order of magnitude deeper than in these maps. This is important, because the 12m observations will then reach low-mass, low-surface column density dust and gas representative of the diffuse ISM, which will not be reached by the Herschel results. This diffuse ISM may be the most susceptible to the processing effects we intend to study.

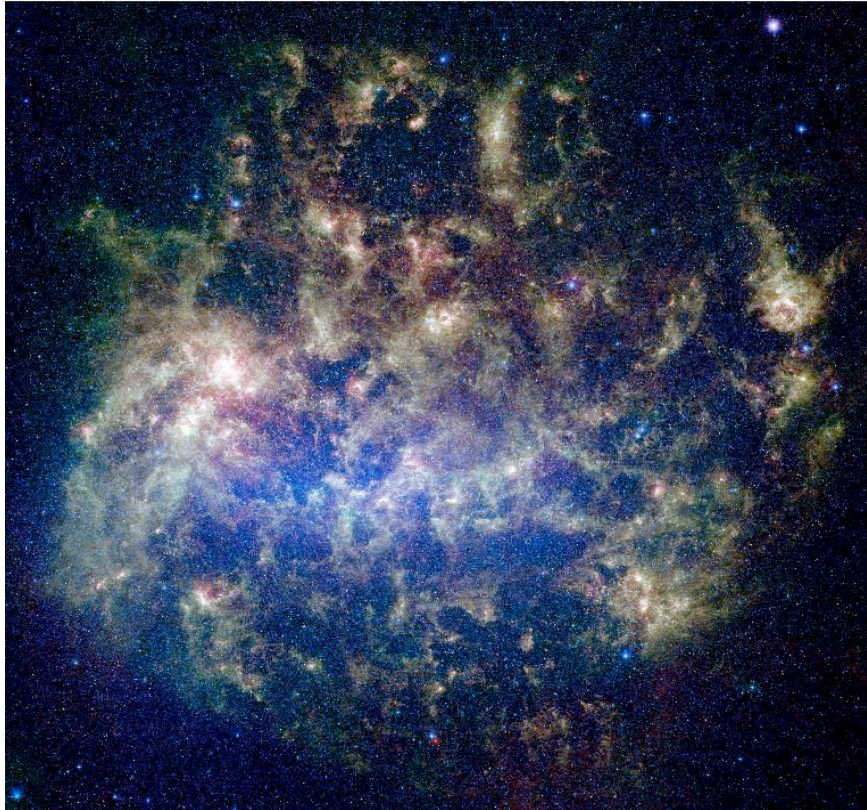


**Figure 4.1:** Multicolour image of the LMC infrared emission shortwards of 200 microns, obtained by the Spitzer Space Observatory. The very filamentary nature of the dust clouds depicted illustrates their sensitivity to the ambient conditions. A full accounting of dust processing is, however, only possible if the dust emission SED longwards of 20 microns is also carefully determined.

Finally, it should be noted that the program would greatly benefit from any larger aperture, e.g. 25 m. This would allow not so much faster mapping, as indeed deeper mapping. Additional channels at 650 microns and 850 microns would also benefit from an Antarctic location, and be especially invaluable in more accurately defining the important submillimetre part of the SED.

## 5 Galaxy evolution

### 5.1 Galaxy Formation and Evolution, the case for a large telescope operating in the FIR

#### 5.1.1 The need for sensitive FIR observations to map the buildup of stars and black holes

As a result of coordinated observations of the best studied cosmological fields, the broad outlines of the assembly of baryonic matter and its coupling to the cosmic energy budget are starting to emerge. Most of the energy from star formation (SF) and active galactic nuclei (AGN) from high- $z$  is absorbed by

dust and re-radiated at infrared wavelengths. Most stars in the universe formed at  $1 < z < 4$  (e.g., Dickinson et al. 2003), and the giant black holes (BHs) in the centers of galaxies also grew most of their mass during that period (Hasinger et al. 2005). The masses of BHs and their host galaxies in the local Universe are closely connected, suggesting co-evolution at high redshift. Current theoretical models invoke the action of AGN to regulate and perhaps terminate SF in massive galaxies (Kaviraj et al. 2007).

However, these processes have only been indirectly studied, and there are few quantitative constraints on the physical mechanisms at work. Nor do we clearly understand high redshift SF. Current measurements of the cosmic SF history over-predict estimates of the stellar mass density at both low and high redshifts (Hopkins & Beacom 2006; Ferguson et al. 2002), suggesting that either the measurements or the stellar population models connecting them are faulty. The mechanisms that govern SF in galaxies are poorly understood: recent evidence points to relatively steady-state growth rather than episodic, merger-driven starbursts, with a tight linkage between galaxy mass and star formation rate (SFR) (Noeske et al. 2007; Elbaz et al. 2007; Daddi et al. 2007a). However, the normalization of this correlation is badly mismatched in theoretical models (Dave et al. 2007). Theory vastly under-predicts the space density of the most rapidly star-forming high- $z$  galaxies (Baugh et al. 2005), and the evolutionary connection between different high redshift galaxy and AGN populations is poorly understood.

These uncertainties are directly related to the fact that observations to date have only been sensitive to a small fraction of the bolometric energy emerging from dusty SF and AGN. Far-infrared (FIR) measurements have been obtained at wavelengths that are too long (submm) or too short ( $< 100 \mu\text{m}$ ) compared to the emission peak, and have not been sensitive enough to detect typical objects -- only rare, hyperluminous sources have been within reach. Observations of emission from typical star forming galaxies detect only a small fraction of their emergent energy, requiring very large and uncertain extrapolations: either from the ultraviolet (UV), where most young starlight is absorbed by dust, or from mid-infrared (MIR) wavelengths, also subject to large bolometric corrections, where the complexity of spectral emission and absorption features and their underlying physics lead to large uncertainties. A direct view of the thermal emission from galaxies responsible for most of the SF and BH accretion at high redshift has eluded us.

Similarly, most of the background emission at its peak wavelengths (Fig. 4.2, right) is still to be resolved in discrete sources, implying that we have not directly detected yet at these wavelengths a large fraction of the sources responsible for the buildup of stars in the distant Universe. As a result, sensitive observations of the 200-450  $\mu\text{m}$  regions would provide ground breaking new science, allowing to measure the peak of the bolometric emission of distant galaxies (Fig. 4.1, left) and thus to reliably estimate the total energy budget of their powering sources. For star forming galaxies, the bolometric emission is a direct measure of the ongoing SFR. Accurate measurements of the bolometric emission in galaxies is crucial also to unveil the presence of highly obscured AGN activity, though to be the dominant mode of BH growth at high- $z$ .

### 5.1.2 Required depths

One can ask, given our current understanding, what is the typical depth that needs to be reached in the FIR in order to address these major scientific questions of the buildup and assembly of stars and supermassive BHs in galaxies, over the  $1 < z < 4$  range. Given the existing correlations observed between stellar mass and SFR, evolving in normalization as a function of redshift (Noeske et al. 2007; Elbaz et al. 2007; Daddi et al. 2007a, see Fig. 4.2 left), it turns out that reaching to galaxies with typical stellar masses of  $\sim 10^{10} M_{\odot}$  is required to obtain a census of most ( $> 2/3$ ) of the stellar mass density and SFR density in the  $z \sim 2$  Universe (Franceschini et al. 2006; Daddi et al. 2007a; Reddy et al. 2008). Within this limits, one expects to include also the bulk of obscured AGN activity due to Compton Thick sources (Daddi et al. 2007b; Fiore et al. 2008).

This maps into the requirement of measuring bolometric emission of sources having  $\text{SFR} \sim 10 M_{\odot}/\text{yr}$  at redshifts up to at least  $z=3$ . Reaching such a goal would correspond to ground-breaking progress in the field, and appears within the possibilities of a 12m facility placed at DomeC, given the expected sensitivities (see table 4.1). We estimate that such galaxies would have fluxes of order of  $1 \sim \text{mJy}$  at both  $350 \mu\text{m}$  and  $450 \mu\text{m}$ , comparable to the expected confusion limit of the 12m facility at these wavelengths. To compare with the best extragalactic surveys of these days, a GOODS-sized field ( $150 \text{ arcmin}^2$ ) could be mapped to full depth using a few months of telescope time; a COSMOS-sized area (2 square degrees) would require a full year of telescope exploitation to reach somewhat shallower flux levels of  $2\text{-}3 \sim \text{mJy}$  (Table 4.1).

## 5.2 Synergies and complementarity to Herschel and ALMA

Herschel (launch beginning of 2009) will soon explore this  $200\text{-}450 \mu\text{m}$  window to unprecedented depths. Its mapping speed at  $350 \mu\text{m}$  and  $500 \mu\text{m}$  with the SPIRE camera will be comparable to that of a 12m facility at Dome C. However, with its 3.5m diameter, Herschel will be very rapidly dominated by confusion noise due to its large beam size, expected to limit surveys to  $\sim 15 \text{ mJy}$  in these bands. Consequently, only the fairly rare ultraluminous galaxies will be detected at these wavelengths (Fig. 4.1, right). Herschel won't be able to measure directly the bolometric output of typical high- $z$  galaxies. Its shorter wavelengths observations with the PACS camera at  $100$  and  $160 \mu\text{m}$  have better resolution and can reach to fainter SFRs (Fig.2, right), but still falling shorter from the necessary depths by about an order of magnitude for mapping  $z > 2$  galaxies. A 12m facility at Dome C would nicely complement Herschel surveys by allowing an order of magnitude depth increase in sensitivity from the bolometric emission of distant galaxies.

ALMA (expected to be in full scale operation by 2015) will allow interferometric imaging down to  $450 \mu\text{m}$ . Thanks to its huge collecting area and exquisite resolution, it is expected to be able to probe to extreme depth down to this wavelength. As a comparison, at fixed observing time ALMA can detect continuum sources 5-10 times fainter than what possible with estimates for a 12m facility at Dome C. However, the primary beam of ALMA antennas at  $450 \mu\text{m}$  is only  $9''$ . As result, the mapping speed of a 12m facility at Dome C at  $450 \mu\text{m}$  is 100 times higher. A similar facility will thus be crucial to survey large samples of distant galaxies measuring their bolometric emission to the required faint levels, and to feed ALMA with the best targets for addressing the open problems in galaxy formation and evolution. Even considering the possibility of ALMA surveys at  $850 \mu\text{m}$  or  $1.2\text{mm}$ , having larger field of views, and the use of photometry at these wavelengths to indirectly derive the bolometric luminosity, would still imply a 50 times lower mapping speed with respect to a 12m facility at Dome C. This also implies that such a sensitive imaging at  $350$  and  $450 \mu\text{m}$  will be crucial also to reliably preselect very high- $z$  ( $z >> 4$ ) galaxy candidates for ALMA observations. Having fairly low space densities ( $< 100/\text{deg}^2$  to levels probed so far), these sources cannot be easily identified at random by means of deep ALMA pointings.

## 5.3 SCUBA2 and related surveys

While there is a clear need for such ultra-deep FIR observations, which will still be important a decade from now, it is not clear if the required goals can be reached from observational sites other than in Antarctica. SCUBA2 at JCMT is claimed to reach comparable NEFD at  $450 \mu\text{m}$  than what estimated here for a 12m facility in Antarctica, but these could be reached on relatively rare occasions on Mauna Kea. A survey is planned to cover  $1.3$  square degree to  $2.5 \text{ mJy}$  depth at  $450 \mu\text{m}$ . These goals might be over optimistic, so far observations from Mauna Kea at these wavelengths have not pushed significantly below  $20 \text{ mJy}$ .

## 5.4 A case for a much larger facility ?

To match Herschel's confusion limit at  $160 \mu\text{m}$  with  $200 \mu\text{m}$  observations with a 12m facility at Dome C would require  $\sim 100$  hours. To beat Herschel at  $200 \mu\text{m}$  and competitively exploit that window

requires a 25m telescope. We emphasize the gigantic leap forward that would be enabled from a 25m telescope (single dish or interferometer): the mapping speed would grow by  $D^2$  (a factor of 4). Even more importantly for extragalactic surveys where the sensitivity is still the major limiting factor, the time to reach a given flux would go down as  $D^4$  (a factor of 16). The much smaller PSF would virtually solve all confusion issues for extragalactic deep fields.

### 5.5 Accessing the best studied fields

A facility in Antarctica could not access some of the currently best studied cosmological field that are either equatorial or in the Northern hemisphere. However, it could access southern fields that could be observed in sinergies with ALMA and existing Southern facilities (Chile, South Africa, Australia). Deep fields in the southern hemisphere already exists (notably, the Hubble Deep Field South and flankign fields, the GOODS-South and Extended CDFS field, the "Marano field").

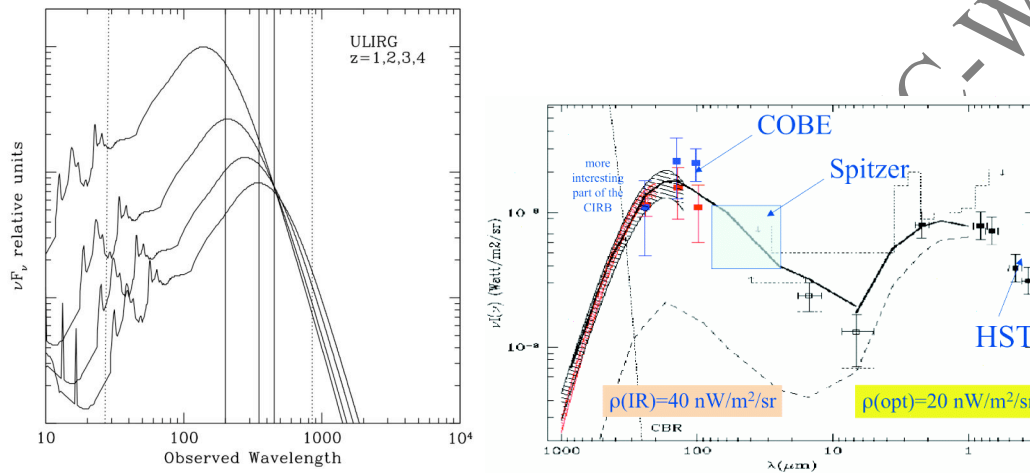


**Figure 5.1.** **Left:** Spectral energy distribution of Ultraluminous IR galaxies (ULIRGs), redshifted at  $z=1,2,3,4$ . The peak of the bolometric emission shifts at 200-400  $\mu\text{m}$  as a function of redshifts, well centered to the wavelengths accessible at DomeC. The dotted vertical lines show the 24  $\mu\text{m}$  (Spitzer) and 850  $\mu\text{m}$  (Scuba, etc) observing wavelengths. **Right:** a recent determination of the extragalactic background light, as a function of wavelength (Franceschini et al 2008). The FIR portion accounts for the largest fraction of the background, and peaks between 100-300  $\mu\text{m}$ . The background at  $>200 \mu\text{m}$  is dominated by distant, cosmological sources and thanks to K-correction effects it is a direct tracer of star formation in the distant Universe.

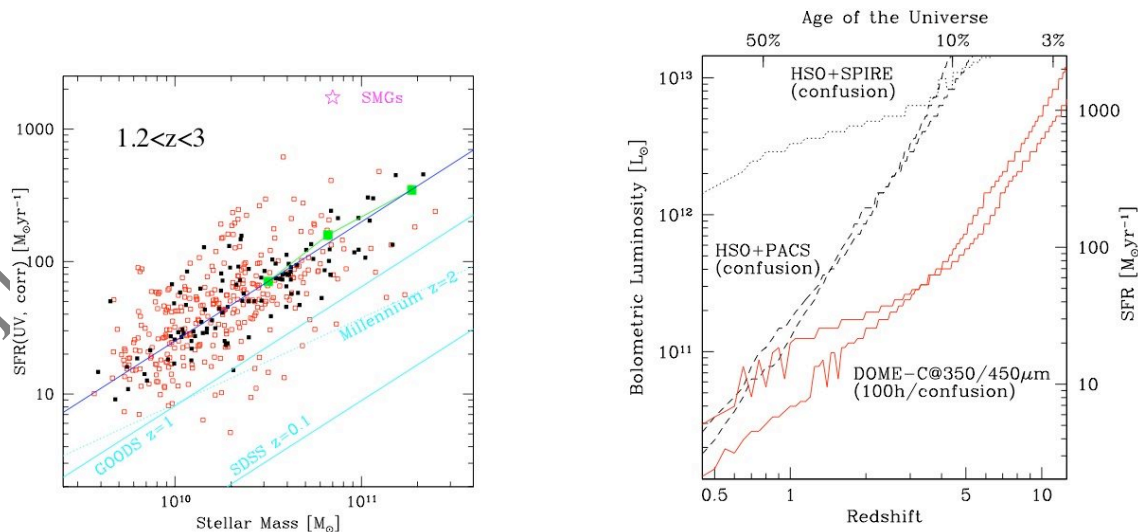


**Figure 5.2.** **Left:** The correlation between stellar mass and SFR in  $z\sim 2$  galaxies (adapted from Daddi et al 2007a). **Right:** Limiting depths for star forming galaxies that can be reached with Herschel PACS

and SPIRE imaging to their respective confusion limits, compared to that of 350  $\mu\text{m}$ +450 $\mu\text{m}$  observations from a 12m facility at Dome C (100 hours of observations of a deep field, mapping 40 arcmin<sup>2</sup> down to  $\sim 1$  mJy at both wavelengths). Flux limits are converted to corresponding bolometric luminosities using the Chary & Elbaz (2001) template libraries.

**Table 5.1:** Extragalactic survey speed: censusing galaxy and black hole mass assembly. We assume coadding 350  $\mu\text{m}$  and 450  $\mu\text{m}$  data for maximum efficiency. SFR limits are for a Salpeter IMF, computed using the Chary & Elbaz 2001 library. Facility speed is estimated assuming 50% of usable time per year and 50% of operational overhead.

Integration (per field)	5 sigma limit (point source)	SFR(z=2) M <sub>⊙</sub> /yr	SFR(z=4) M <sub>⊙</sub> /yr	Facility speed deg per yr
100 h	1 mJy	$\sim 20$	70	0.2
10 h	2.5mJy	$\sim 70$	$\sim 200$	2.0

## 6 Far-infrared and submillimeter spectroscopy of galaxies along their evolution

One of the most important astrophysical questions that still has to be answered is *how galaxies evolve from the first structures to the present day*. A great effort has been done with the cosmological surveys of ISO, Spitzer and ground-based submillimeter telescopes (eg the SCUBA surveys at JCMT). In the incoming years, Herschel will devote a large amount of time to deep and shallow surveys. The approach is to observe deep fields in a few photometric bands to derive the logN-logS distributions, build the spectral energy distributions to be used -together with models- to distinguish among the various types of galaxies (spheroids, ellipticals, starburst or AGN) at different redshifts. Follow up spectroscopic work from ground-based telescopes is then used for accurate redshifts. The limitation of this approach is however the lack of detailed information on the physical processes dominating the energy budget, making any conclusion on the nature of the observed objects very model dependent.

Only spectroscopic surveys at different redshift, at the wavelengths where the bulk of the energy is emitted (mid-to-far infrared) will be able to identify the energy production mechanisms during their evolution and therefore their nature. This will shed light into the role of AGNs and starbursts along galaxy evolution. We know that the main energy-generating mechanisms in galaxies are black hole accretion and star formation and that starbursts and AGNs may be linked in an evolutionary sequence. On a cosmic scale, the evolution of supermassive black holes is tied to the evolution of the star-formation rate (Marconi et al 2004, MNRAS, 351, 169; Merloni et al 2004, MNRAS, 354, 37).

Also on a local scale *star formation* and *nuclear activity* are linked. The possible evolutionary scenario is: HII galaxies  $\rightarrow$  Seyfert type2 (Storchi-Bergmann et al 2001, ApJ, 559, 147), or extended to: HII galaxies  $\rightarrow$  Seyfert 2's  $\rightarrow$  Seyfert 1's (Hunt & Malkan 1999, ApJ, 516, 660). In this scheme, starburst emission is first triggered by galaxy interactions, leading to the concentration of a large gas mass in the circumnuclear region of a galaxy. Later, mergers and bar-induced inflows can bring fuel to a central black hole, stimulating AGN activity.

Given the above scenario, *we want to understand galaxy evolution through the history of the luminosity source of galaxies*. The observational approach is based on mid-to-far IR and submillimeter spectroscopy, able to derive the bi-variate AGN and Star Formation luminosity functions at various cosmic epochs, from the Local Universe to high redshifts. The spectroscopic diagnostics will include the typical AGN tracers (high ionization lines) and star formation tracers (HII regions lines and low-ionization or neutral lines, such as the [OI] and [CII] far-IR transitions).

This observational goal can be reached at Dome C with a large (12m to 25m) submillimeter telescope, operated in the submillimeter windows in particular at 200 $\mu\text{m}$ , 230 $\mu\text{m}$  and 280 $\mu\text{m}$  - which open only at Dome C when the precipitable water vapor (PWV) content of the atmosphere reaches levels of the order of 0.1-0.2mm. At these low levels of PWV also the mid-IR (in the range of 10-40 $\mu\text{m}$ ) atmospheric windows open and mid-IR observations can be collected, provided that the submillimeter



telescope has an inner part (3-4m) of its mirror optically worked. This dual channel observatory will collect imaging and spectroscopic data with comparable beam sizes at 10-40 $\mu\text{m}$  and 200-350 $\mu\text{m}$  of galaxies at increasing redshifts.

**What are the spectroscopic tracers?** Mid-IR and submillimeter spectroscopy can trace both the AGN (photoionization from non-thermal processes) and the Star Formation component (stellar photoionization, shocks, PDRs - photodissociated regions), through fine-structure emission lines not suffering extinction that obscures the galactic nuclei both locally and at cosmic times.

Fig. 1(left) shows the very large density-ionization plane that can be traced by infrared fine-structure lines, which are good diagnostics for gas densities of  $10^2 \rightarrow 10^8 \text{ cm}^{-3}$  and ionization potentials up to 350 eV. The critical density (i.e. the density for which the rates of collisional and radiative de-excitation are equal) of each line is plotted as a function of the ionization potential of its ionic species. This diagram shows how these lines can measure the two fundamental quantities (density and ionization) of the gas. Lines from different emission regions are shown in different loci. The ratio of two lines with similar critical density, but different ionization potential, measures the ionization, while the ratio of lines with similar ionization potential, but with different critical density, can measure the density of the gas (see eg: Spinoglio & Malkan 1992, ApJ, 399, 504). The identified emission line regions span from neutral or weakly ionized regions, such as PDR at the interface between HII regions and molecular clouds, HII regions excited by young stars, Narrow Line Regions excited by the AGN and the so-called Coronal Line Regions with the highest ionization lines, originated from the high energy photons emitted during the AGN accretion process.

Considering the three local galaxies M82, NGC1068 and NGC6240 as template objects, we computed the line intensities expected at redshifts ranging from 0.1 to 5. For simplicity, we adopted an Einstein-De Sitter model Universe, with  $\Omega_\Lambda = \Omega_{\text{vac}}=0$  and  $\Omega_M = 1$ ,  $H_0=75 \text{ km s}^{-1} \text{ Mpc}^{-1}$ . The luminosity distances have been derived using:  $d_L(z) = (2c/H_0) [1+z - \sqrt{1+z}]$ . The results are reported in Fig. 1(right), where the line intensities are given in  $\text{W m}^{-2}$  and the expected sensitivities of the Herschel PACS spectrometer are reported. We have assumed that the line luminosities scale as the bolometric luminosity a luminosity evolution proportional to the  $(z+1)^2$ , consistent with the Spitzer results at least up to redshift  $z=2$  (Perez-Gonzalez et al. 2005).

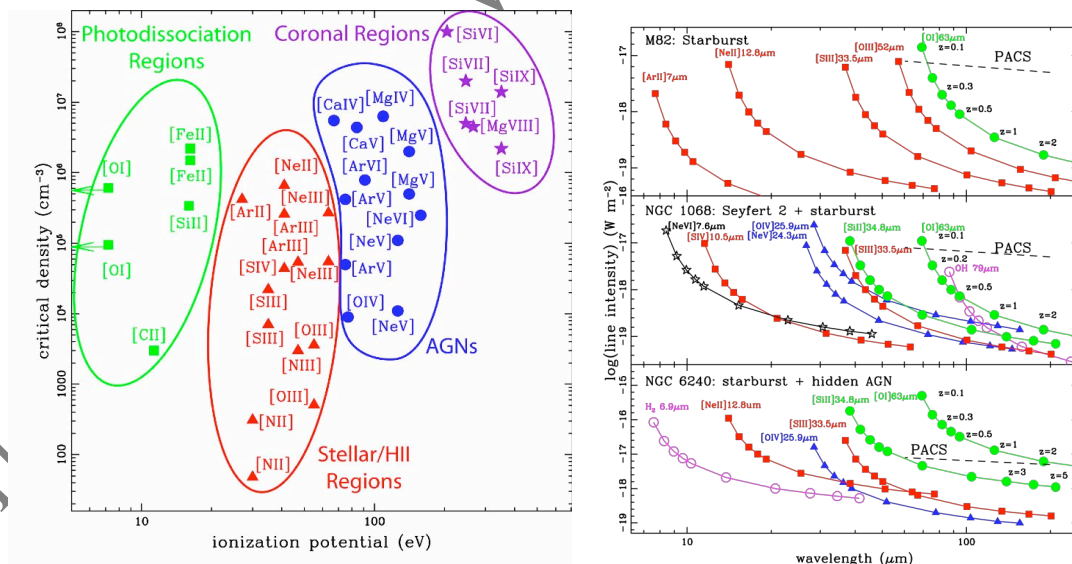


**Figure 6.1** (a) Left: Fine-structure lines in the 3-200  $\mu\text{m}$  range, plotted as a function of their ionization potential and critical density. Different areas identify different physical regimes (b) Right: Predicted line fluxes as a function of redshift, using three local templates. Squares indicate the fluxes of HII region lines, triangles the fluxes of lines emitted by AGN, filled circles the fluxes of the [OI] and [SiII] lines and open circles molecular lines (from OH and  $\text{H}_2$ ).

## 7 A potential case for Dome C: the Sunyaev-Zel'dovich Effect

### 7.1 Introduction

A large amount of information in Cosmology has been derived, and is still under analysis, through observations of the primary anisotropies of the Cosmic Microwave Background (CMB), the tiny fluctuations in temperature, reflecting the density ones, present at the epoch of transition when CMB photons decoupled by neutral matter at redshift  $\sim 1100$ . The energy/matter budget of the universe has been partitioned in a 5% of baryonic matter, a 25% of dark matter and a remaining of 70% of dark energy to allow a flat universe with a present density close to the critical one, as it results from observations [de Bernardis et al. 2002, Komatsu et al. 2008].

A promising science, that is having by right a key role in the so called Precision Cosmology Era, is the study of the secondary anisotropies of the CMB. We observe today the CMB photons as they left the last scattering surface but after travelling to us and so interacting with all the matter along their path through the universe. These interactions have generated the secondary anisotropies that we can discriminate on the basis of the two main families of matter & radiation interactions: by gravitational potential wells and by scattering. We focus on one of the second family.

The Sunyaev-Zel'dovich Effect (SZE) is the distortion induced into the CMB spectrum by the energy transfer due to Thomson scattering of CMB photons by hot gas. The observed anisotropy is at the scale of galaxy clusters and superclusters, even if it may also be produced on very small scales by the first stars in the universe [Sunyaev & Zel'dovich 1972, 1980; Rephaeli 1995, Birkinshaw 1999, Carlstrom, Holder & Reese 2002]. The SZE is known as a nuisance factor to cosmological parameter extraction from measurements of primary CMB anisotropies, but it is a potentially powerful tool for cosmology. Accurate spectral and spatial observations makes the SZE a *radial speedometer* and an efficient *mass finder* both in a direct way for baryonic matter (visible or dark), and in an indirect way for non baryonic dark matter. The peculiar independence of this effect from the redshift of the scattering source allows observations of far away targets avoiding the brightness reduction present in visible and X-ray spectral ranges surveys.

The thermal component (th-SZE) is a CMB spectral distortion due to the inverse Compton interaction between the CMB photons and free electrons of a hot ionised gas along the line of sight. The result is a net energy transfer from photons in the Rayleigh-Jeans tail of the CMB spectrum to the Wien tail. The cross-over frequency, corresponding to a null distortion, is around 217 GHz but a weak dependence of this value on the gas temperature is also present.

The kinetic Sunyaev-Zel'dovich Effect (k-SZE) is the component due to the Doppler effect caused by the bulk motion of the electron gas that scatters the CMB photons. In the non-relativistic regime it causes no spectral distortion, maintaining a planckian spectrum, therefore resulting a challenging detection because it is impossible to disentangle from primary CMB anisotropy at the same angular scales. In the case of angular scales corresponding to multipole index larger than  $l \geq 2500$  (*i.e.*  $\theta \leq 5$  arcminutes) SZE components dominate CMB fluctuations as shown in Fig.6.1.

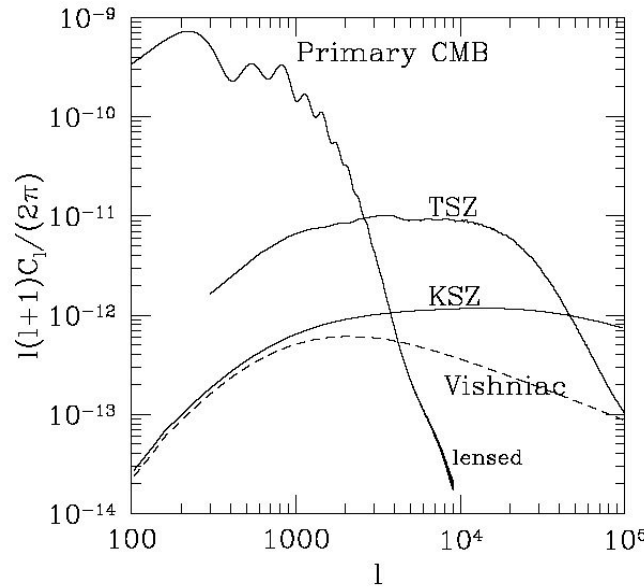


**Figure 6.1** - Thermal and kinetic SZE power spectra as deduced by numerical simulations compared with CMB power spectrum. The results include non-linear regime and are obtained by assuming universe was reionised at  $z = 16.5$  and remained ionised after that [Zhang, Pen & Trac , 2004].

Relativistic corrections have to be considered in the presence of hotter and denser scattering media [Itoh et al. 2002; Shimon & Rephaeli 2002]. Non-thermal populations of electrons can also contribute as a different components to the SZ spectrum [Colafrancesco, Marchegiani & Palladino 2003]. The main components of SZE are shown in Fig.6.2 with the expected atmospheric windows from Dome C assuming optimum observational conditions with a pwv equals to 0.1mm.

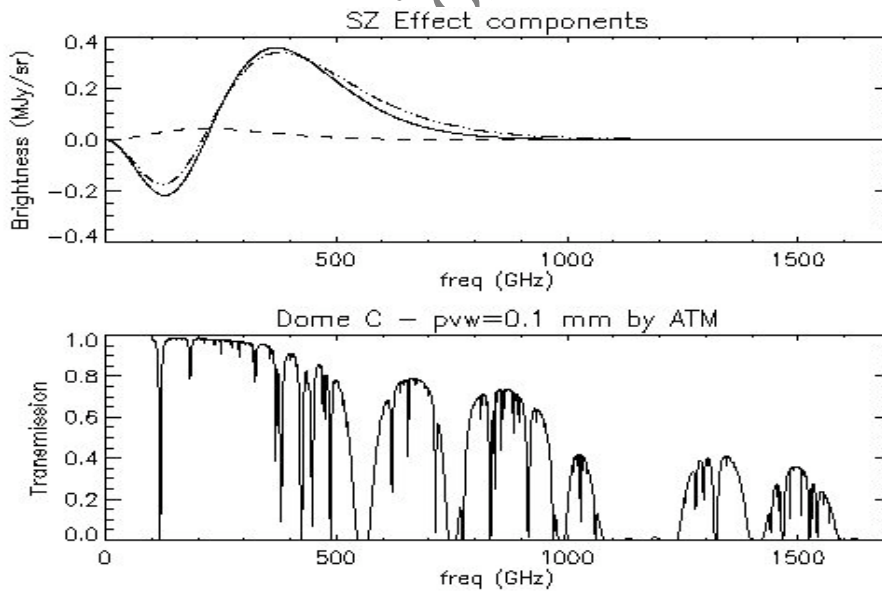


**Figure 6.2** – *Upper panel*: SZE spectra splitted in thermal component (solid line), kinetic component (dashed line) and all the components with relativistic corrections (dot-dashed line). *Lower panel*: transmission at Dome C as derived by ATM programme considering a precipitable water value equals to 0.1mm.

The SZE is mainly caused by the pressure of free electrons of hot ionised gas entailing that intracluster gas (IC) is the most favourite ambient. In this way SZE blind surveys allow to count all the clusters of galaxies which do not exhibit an alternative visible counterpart. Having the instrumental capability to detect high redshift clusters (*i.e.* sensitivity and angular resolution) gives the possibility to reconstruct the evolution of this structures allowing to put constraints to cosmological parameters such as the amount of dark energy and its equation of state (see Fig.6.3).

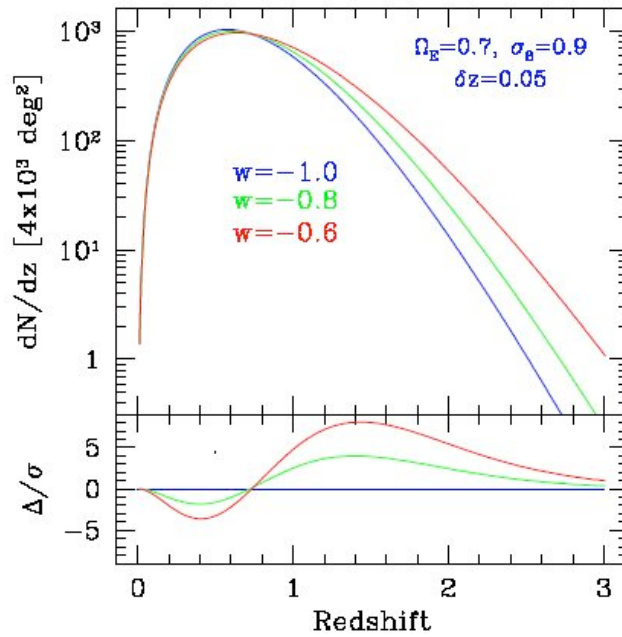


**Figure 6.3** – The cluster redshift distribution for a 4000 deg<sup>2</sup> SZE survey proposed for the South Pole is sensitive to the dark energy equation of state  $w$ . Three models with different  $w$  are shown (above) and statistical differences quantified (below) [ Mohr 2005]

Anyway we have to highlight that SZE takes place in all astrophysical environments where both the conditions of ionisation and high temperature are fulfilled at the same time. Hydrodynamical simulations show that diffuse matter in the phase of warm-hot gas ( $T_e=10^5-10^7$  keV) is expected to be present in large structures in the form of filaments. This gas might account for a fraction of the missing baryons in the universe [Fukugita, Hogan & Peebles 1998]. The th-SZE of this gas is really low and comparable to the k-SZE component; even if the SZE luminosity is low this is a valid alternative for searching missing baryons.

An interesting scientific goal derived by SZE observations is the extraction, together with other cluster parameters, of the temperature of the CMB photons at cluster redshift allowing the monitoring of the CMB temperature evolution [see Battistelli et al. 2002 for the first observational approach].

Targets for SZE can be distinguished between observations of individual clusters, in order to collect a large sample of them, and wide blind surveys for statistical approaches.

The expected results can be summarised as in the following:

- reconstruction of the Hubble diagram for deriving cosmological parameters;
- counting clusters along the redshift for deriving cosmological parameters;
- estimate of baryon mass fraction;
- measuring CMB temperature along the Universe.

More challenging results are:

- detection of missing baryons;
- mapping of radial peculiar velocities of galaxy clusters for constraining dark energy parameters.

## 7.2 Peculiarities for Dome C SZE observations

The site allows observational conditions common with other scientific objectives; mainly resulting in excellent measurement conditions for the mm-FIR spectral range from ground. The possibility of performing simultaneous observations in all atmospheric windows between 200  $\mu\text{m}$  and 2 mm allows deep integration towards sky regions with high angular resolution and large spectral coverage.

FWHM=BT (arcmin)	$\delta T_{rms}$ ( $\mu\text{K}$ )	$ v_{min} $ (km/s)
0.1	2.1	46
0.2	4.2	93
0.3	6.3	138
0.4	8.3	184
0.5	10.3	227
1	19.4	426
2	32.2	708
3	39.6	871
4	44.1	969
5	46.9	1033
6	49.1	1079
7	50.8	1117
8	52.2	1149
9	53.4	1175
10	54.4	1196

**Table 7.1** – Estimated CMB temperature dispersion considering a double beam differential sky observations with a beamthrow (BT) equals to the field of view (FWHM). The correspondent cluster peculiar velocity along the line of sight is converted assuming an electronic optical depth equals to  $5 \cdot 10^{-3}$ .

The SZE spectrum does not show spectral features demanding high spectral resolution and so the possibility of observation by multi-frequency photometers or by spectrophotometers is allowed.

A large dish telescope (12-m or more in diameter) allows the possibility to carefully explore far away Universe looking for clusters of galaxies by blind surveys. An high angular resolution, difficult to reach by a satellite instrument, (*i.e.* fov=24" FWHM @ 1.4mm, the cross-over wavelength) ensures an accurate mapping of the morphology of large clusters. A reduced contamination by primary CMB anisotropies opens the exploration of k-SZE observations. See in Tab.6.1 the reduction of CMB confusion, converted also in the minimum detectable cluster peculiar velocity, as decrease the field of view (FWHM). A double beam differential sky observations are considered with a beam-throw BT equals to the fov.

A multi-frequency observation of the full SZE is mandatory for an efficient extraction of gas parameters: electrons density and temperature and cluster radial peculiar velocity. For this purpose extending the observations to high frequencies allow to sample the intracluster dust emission disentangling this contamination from SZE spectra at low frequencies.

An accurate forecast of confusion by mm/FIR point sources is requested. It is often pointed out that mm/submm surveys may suffer from strong confusion limits due to the tail of IR emission from unresolved compact objects (active galaxies and spheroids). A precise evaluation of these confusion limits is therefore critical to fully assess the capabilities of a facility to operate at given wavelengths in presence of strong contaminating fluxes integrated on its field of view. This evaluation is dependent on the assumed model for the source distribution (with special regard to the clustering phenomena) and, of course, on the limits set by the angular resolution of the telescope [Lapi et al. 2006; De Zotti et al. 2005; Negrello et al. 2007]. In Table 6.2, we show the scaling of the confusion limits for reference microwave frequencies observable from the ground, for a well assessed source distribution model, as a function of the telescope aperture. It is clear that the choice of large aperture telescope like the proposed 12m facility from Dome C can provide a significant leap forward in SZ science by providing smaller levels of spurious contamination from unresolved compact objects.

frequency (GHz)	1 $\sigma$ confusion limit (mJy)
140	0.46
217	0.63
270	0.84
350	1.00

**Table 7.2** – Confusion limits at low frequency bands assuming a diffraction limited field of view for a 12-m in diameter telescope aperture.

Accurate predictions about the results and the observational strategy can be provided when a dedicated focal plane instrumentation will be planned: *i.e.* mm/sub-mm spectrophotometer with imaging capabilities.

## 8 Unique science case: Understanding Sun coronal mass ejection

### 8.1 Impact

Synchrotron radiations are emitted during Sun coronal mass ejections and are usually observed in the microwave part of the spectrum. Understanding this phenomenon will shed light on the physical mechanisms that are responsible for coronal mass ejections such as particle acceleration from the photosphere.

Recent results obtained at submm wavelengths have revealed another potential synchrotron radiation spectrum (Fig. 7.2; Kaufmann et al. 2004). This new spectral component discovered with fluxes increasing for shorter submillimeter wavelengths may indicate that the submm emission is created by particles accelerated to very high energies.

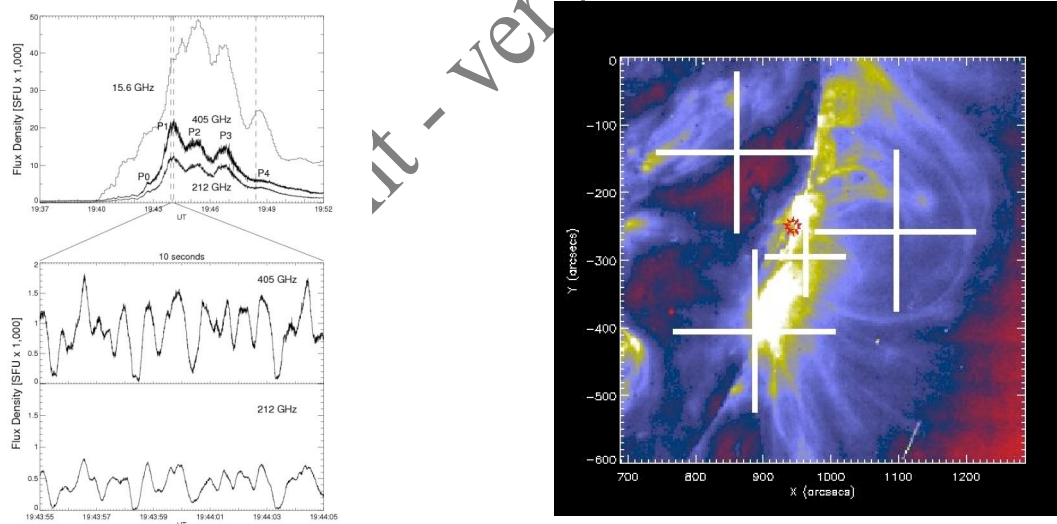


**Figure 7.1:** Left : Time profiles of the Solar burst in November 2003. The 405-GHz emission is more intense than the 212-GHz emission, suggesting a possible maximum in the submm/far-infrared domain. Right : Position of the submm observing beam on the SOHO UV image of the Sun. (from Kaufmann et al. 2004).

First emission models assume three different mechanisms which may become comparable in importance: (a) synchrotron radiation by beams of ultrarelativistic electrons; (b) synchrotron radiation by positrons produced by nuclear reactions arising from energetic beams interactions at dense regions close to the photosphere, and (c) Langmuir waves emission from deep photosphere excited by high energy electron beams (Kaufmann et al. 2006).

Overall, these new results indicate that key questions regarding the physical mechanisms at the origin of solar flares are expected to become better understood with measurements in the far to mid-infrared range.

## 8.2 Other facilities

The Solar Submillimetre-wave Telescope (SST) is located in Argentina at an altitude of 2550m. It is a 1.5m-diameter Cassegrain telescope that can observe at 212 and 405 GHz, which convert to 1.5 mm and 750  $\mu\text{m}$ , respectively. The FWHM beams are 2 and 4 arcmin in these two respective channels. Observations of the Sun require good atmospheric conditions at 2550m despite the large Solar flux density in the submm ( $>10,000 \text{ Jy}$ ) because the atmosphere may become opaque at these wavelengths. Observations with SST have revealed submm bursts in the Solar corona that were associated to the large solar flares in November 2003 (Fig. 7.1).

The current limitation of the SST is the quality of the atmosphere and the corresponding transmission. Observations at 200  $\mu\text{m}$  are basically impossible from the SST site in Argentina. Observations from 500  $\mu\text{m}$  down to mid-IR are important to understand whether incoherent synchrotron radiations are the main mechanisms that generate submm flares (Fig. 7.2). Space is an option with instrument operating at both 150 and 35  $\mu\text{m}$  (e.g. SMESE/DESIR project) but it will be limited in time and in sensitivity. The SMESE bolometers will not be cryogenically cool down. Only major flares with respect to the thermal emission of the Sun will be detected. A second limitation of SST is its size that does not allow high angular resolution observations on the Sun ( $<1 \text{ arcmin}$ ).

Another option is a 2-m class telescope at Dome C in Antarctica. It could operate at both 30 and 200  $\mu\text{m}$ . Given the large flux of the Sun at these wavelengths, observations during day time with only PWV=0.3 mm should be possible. Cryogenically cooled detectors should allow detection of minor flares in intensity. Secondly, a 2-m class would offer a better angular resolution to disentangle the potential sources of flares on the Sun (see Fig. 7.2). A higher angular resolution, and therefore a larger telescope than 2 m in diameter, is not necessary for observing the Sun.

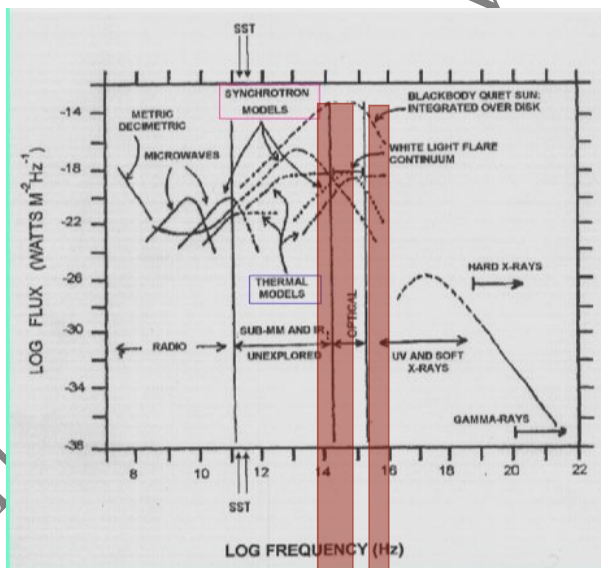


**Figure 7.2** : Spectral energy distribution of Sun emission. Synchrotron radiations from the Sun are expected in microwave and submm bands. Incoherent synchrotron radiations are predicted to be observable with a 2-m class telescope for submm and mid-IR bands (red stripes).

## 8.3 Observations and requirements

To perform submm observations of the Sun, we propose to install a 1000-pixel bolometer array on a 2-m class telescope that could operate at both 200 or/and 350  $\mu\text{m}$ . It could be used either on a monitoring mode or as a follow-up imager if a flare is detected in the visible and UV.

Complementary observations in the mid-infrared would also constrain the spectral energy distribution of the incoherent synchrotron radiation. A 2-m class telescope as Sun corona mass ejection observer will be highly complementary to the Murchison Widefield Array (MWA) in Western Australia whose main goal is to constrain the magnetic field strength during Sun coronal mass ejections.

Special optical filters or shield should be installed in front of the telescope or across the dome aperture for observing the Sun in the submm with a 2-m class telescope.

*Working document - version 1.0 - CMC-WG meeting*



## CHAPTER 2: SITE TESTING

### 9 PWV from atmospheric transmission measurements

A major obstacle to carry out submm observations below 500 microns from ground is the atmosphere as well as the harsh environment of the potential Earth site (high altitude deserts; Antarctica). Preliminary meteorological studies and atmospheric transmission models tend to demonstrate that Dome C might offer atmosphere conditions that open the 200- $\mu\text{m}$  windows. The SUMMIT submm tipper, a collaboration between CEA Saclay and UNSW/Sydney, has started operating in early 2008 for measuring sky opacity at 200 microns.

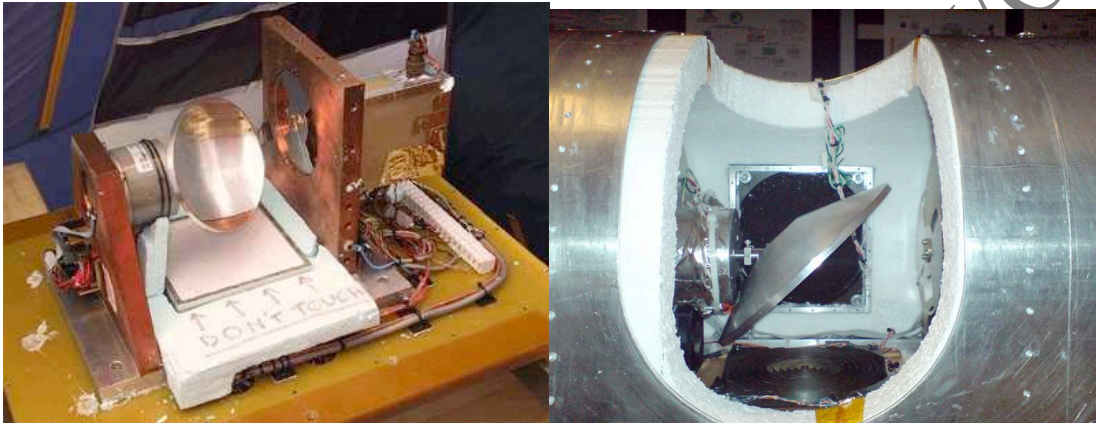


**Figure 9.1:** SUMMIT. Left: Inside with the mirror and the chopper wheel. Right: For 2008 campaign at Concordia the warm black body is kept warm in the airflow, heated by resistors. The reference black body at the rear is in contact with the cold aluminum cover.



**Figure 9.2:** SUMMIT in operations at Concordia with Cochise at the rear.

SUMMIT has been operating since March 2008 and works perfectly at Concordia. Data are available from the beginning of April until now, the preliminary results are given in figure 9.3

Using the Atmospheric transmission model of N. Schneider, it is possible to estimate the transmission at 350  $\mu\text{m}$ .

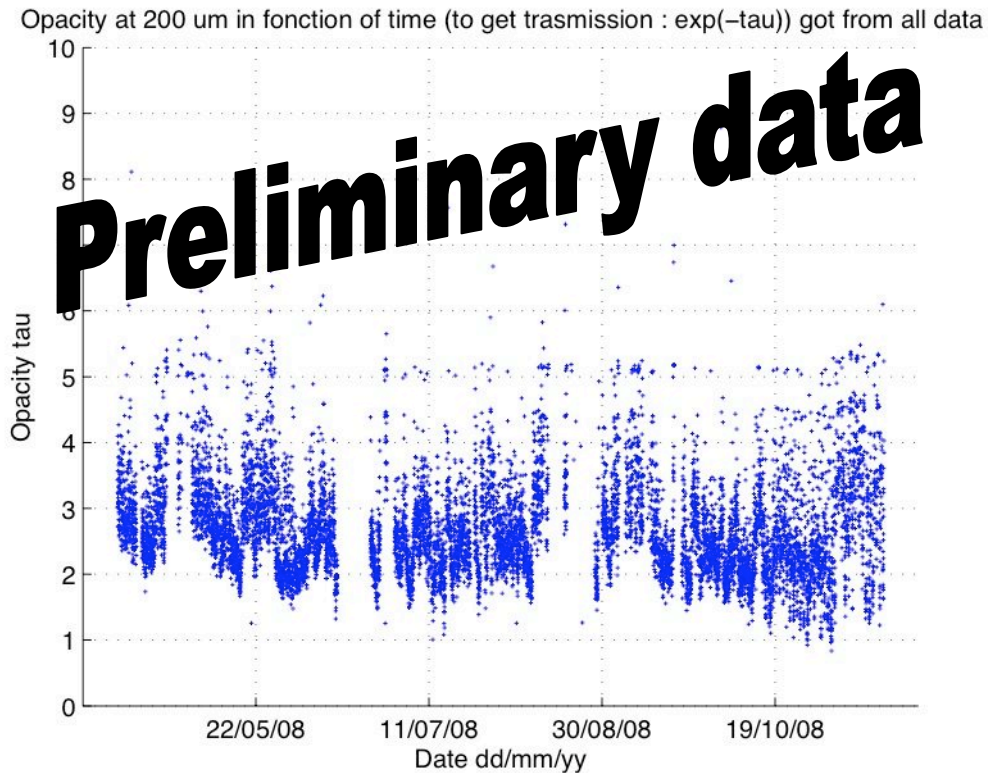


**Figure 9.3:** Opacity of the atmosphere at 200  $\mu\text{m}$  at Dome C between April and December 2008. The transmission is  $\exp(-\tau)$ .

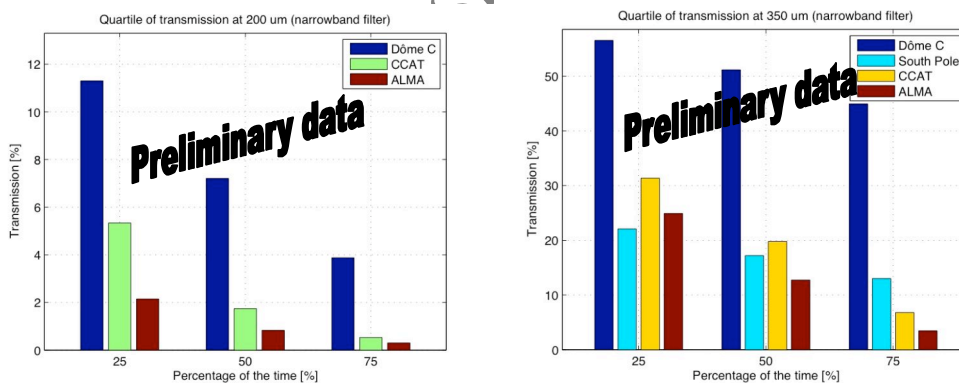


**Figure 9.4 :** Percentage of time the atmosphere has a certain transmission at 200  $\mu\text{m}$  (measurement) and at 350  $\mu\text{m}$  (extrapolated ). The results for Dome C are compared with other sites like Cerro Chajnantor (CCAT site) and Llano Chajnantor (ALMA site) in Chile.

## 10 Thermal gradient and variabilities up to 46 m high

Common prerequisites for the design of unmanned telescopes at altitudes up to 46 m include the ongoing measurements of wind, humidity and temperature. The CEA team currently performs these measurements. The probes consist of 2 horizontal disks (CD like) distant by 10 mm to be used as sun shields. They are black inside, polished aluminium up and down. They are defrosted every 2 minutes for duration of 2 minutes. Inside is placed a thin aluminium cylinder (height 8mm,  $\varnothing$ 10mm) equipped with a Pt1000 small sensor and a small heater (0.25W) working together with disks heaters. The temperature sensor is read every 10 seconds continuously. Turbulence and air temperature stability might be derived afterward.

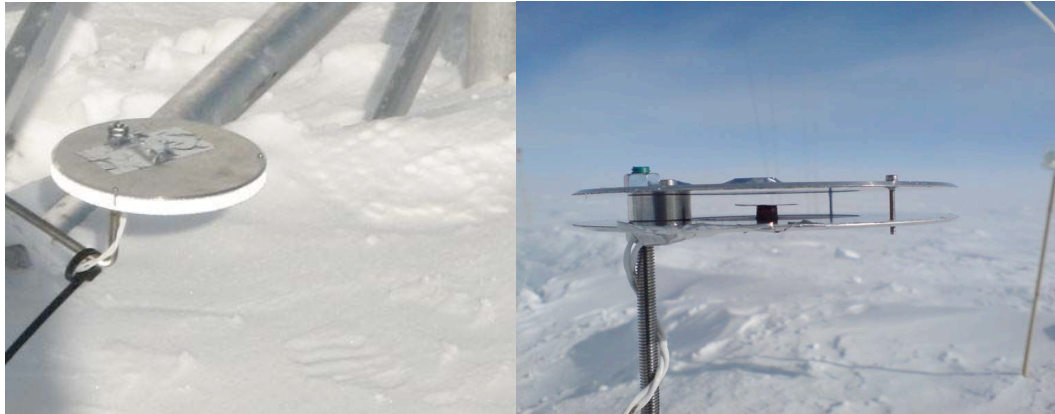


**Figure 10.1:** Left: Shielding of the thermal probes, the sunlight is back-reflected by the lower disk and forward reflected by the upper disk. Right : Pt1000 mounted on a  $\varnothing 20\text{mm}$  disk protected by  $\varnothing 150\text{mm}$  disks.

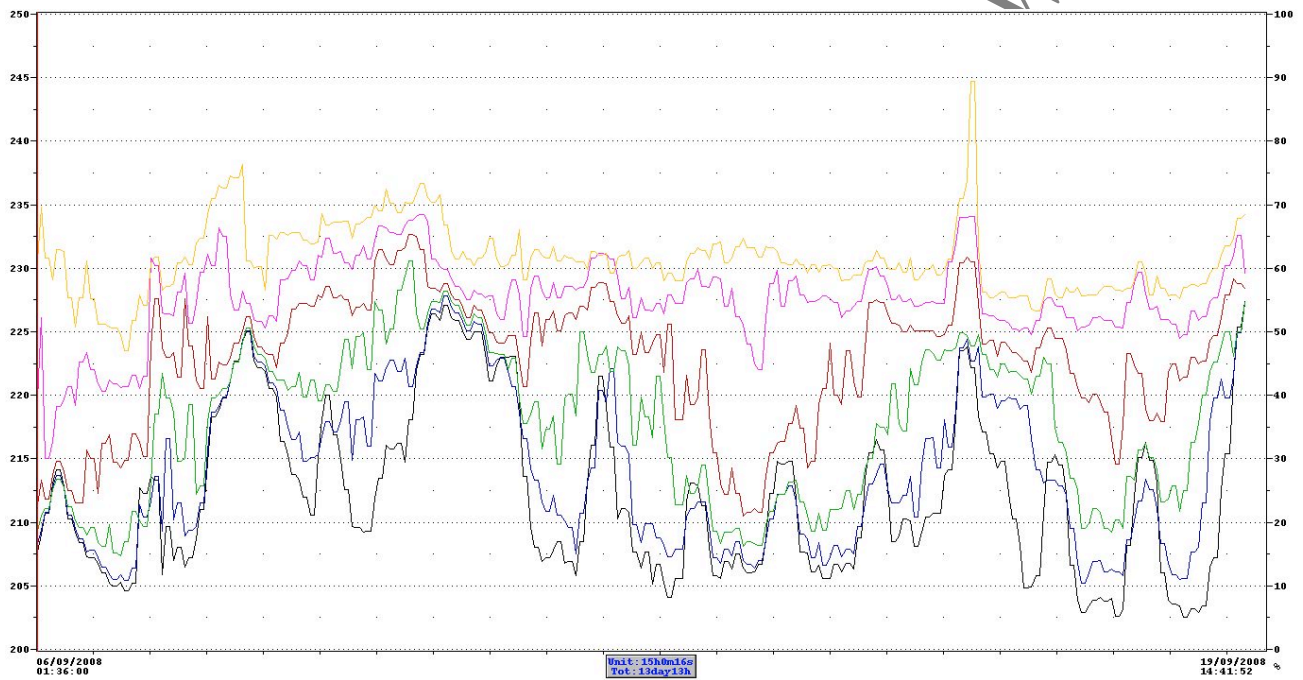


**Figure 10.2:** Temperatures in K measured at 0.2m, 2, 5, 12, 24 and 46m. Note that temperatures are lower at 0.2 m than at 46 m high. Variations of temperature with height go up to 20 K. Besides the temperature at 46m is rather stable compared to the temperature at 0.2m.

Working document

WG meeting

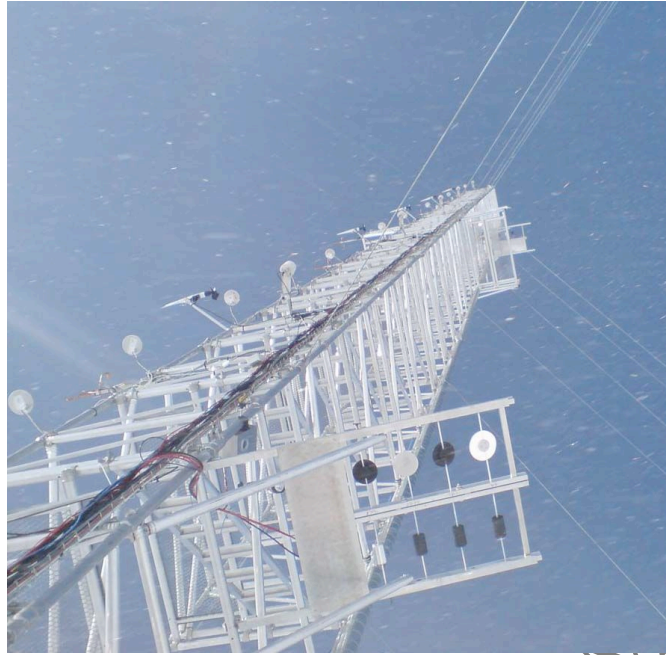


**Figure 10.3:** The temperature cells can be seen on the left of the tower. The frost cells are placed on two platform at 5m and 30m on the right of the 46m mast.

## 11 Frost formation

Dome C climate conditions severely impact and deform any telescope mirror and hardware. Whatever the telescope at Dome C the combination of little wind and high heat lost by radiation during the polar winter, results into a large thermal inversion and strong icing on all hardware objects. The CEA team currently tests different ways of protecting the instruments against frost.

16 temperature and wind measurements are performed from 0 to 46m, with closer altitude resolution near the ground. On an aluminium blade, we shall blow a 0.4x0.6 m<sup>2</sup> glossy aluminium disk with fresh air blown from the ground in order to check if dry air may clean a surface in altitude (Figure 7).



**Figure 11.1:** Left: At 30m a shiny aluminium surface is blown with dry air from the ground level, near the 3 heated frost cells. Right: At 30m up to 6°C above ambient are sometimes needed to keep the cells clear of frost. The blower is not active on this photo. The crystals are typical frost built-up.

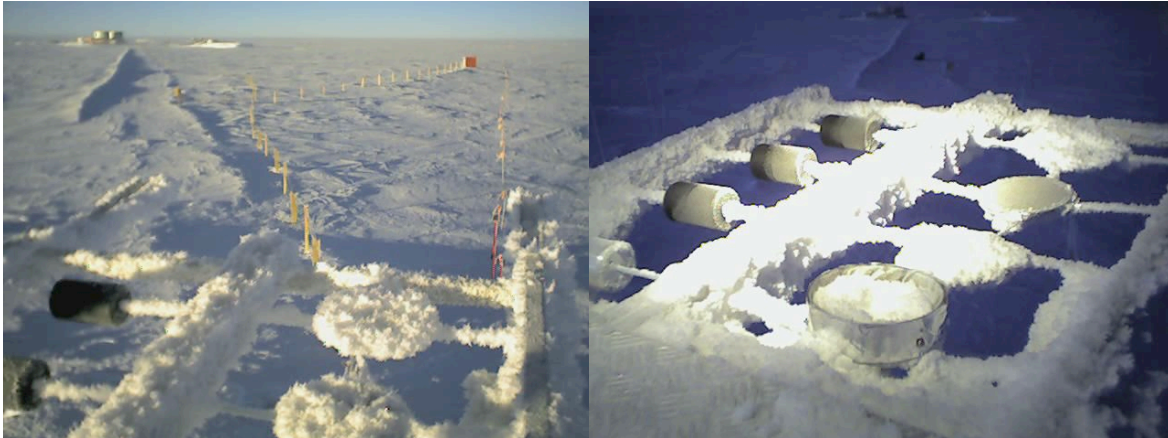


**Figure 11.2:** Left: On 17 april 2008, the frost has covered all the non-heated areas at 5m altitude. A heater at 3°C above ambient is needed to protect from frost built-up. Right: At 5m altitude a disk is surrounded by a heated ring to protect ice built-up on a simulated telescope. On this view the warming up of the ring T ambient + 3°C cannot stop the ice.

The COCHISE telescope (Roma 3 University) has been equipped by a system that will monitor the formation of frost on the telescope primary mirror and will try to stop its formation by heating for instance (Figure 9).

The measurements in process at Concordia will describe how much the air is super saturated at 5m and 30m. The strong temperature gradient blocks the air mixture. During 2007 winter campaign, the frost probes at 7m-altitude indicated super saturation of 75% above 100%. This is highly important as frost forms very quickly at Dome C on any piece of hardware. In the perspective of unmanned telescopes during polar winter, automatic removal of frost will be necessary for all type of telescope.



**Figure 11.3:** Left: The Italian 2.6m telescope Cochise equipped with infrared heaters, 24 holes to blow dry air and a heating system on the mirror. An efficient combination is a small warm up of the telescope to make the surface slippery in addition to blowers to flush the snow. Right: The infrared heaters remove the snow from the M2 support. This unprotected mirror accumulates frost toward the bottom. The M1 mirror in horizontal position is nearly clean. By tilting it, the snow would fall down.



**Figure 11.4:** Left: On this web-cam photo, the mirror is heated 5°C above ambient. The snow is pushed toward the centre of the mirror by both gravity and the blower. Right: Without a cleaning anti-frost system, the mirror is rapidly covered with frost and snow.

Working document - version 1.0 - CMC-Working Meeting

# CHAPTER 3: TELESCOPE FACILITY

## (in partnership with EIE and Thales Alenia Space)

The AST-25m telescope would provide a large collecting aperture with high surface accuracy ( $< 12$  micron) to operate at wavelengths as low as 200 micron, providing deep, high resolution ( $< 2$  arcsec) images. The combination of the transparency at Dome-C and the large aperture would make this the most sensitive submm telescope ever planned. ASO-25m would enable Italy and France (and Europe as a consequence) to be at the forefront of astronomical research and would favour state-of-the-art instrumental development.

Note: telescope specifications and requirements are currently discussed with the industrial partnership. Details will be provided in 2009.

### 12 Top-Level Requirements

This document presents ONLY the top-level design or performance capabilities needed to meet the science goals of this project. The science objectives require a 25m aperture to operate at submm wavebands. Efficient operation at 200 micron implies the net effective surface error be less than 10-12 micron and that you be able to find and track a source with an accuracy of better than 0.2 arcsec. Therefore, there are four main critical areas that still need to be very carefully analyzed and discussed:

#### 12.1 Active Surface

Fabricating, setting and maintaining a 10 micron surface on a 25 m diameter radio telescope is probably the most difficult challenge for this Project. It also implies that active surface control would be necessary. Because the thermal distortions will be very critical at Dome-C it may be necessary to implement a dynamic *closed loop* control system using sensors and feedback. This is commonly done at optical/infrared wavelengths using edge sensors and optical instruments that measure the wavefront errors in real-time.

#### 12.2 Optical Design

The optical design of the telescope is determined by optical, mechanical and focal plane instruments constraints. It must enable efficient operations in the defined wavelength range and field of view (10-20 arcmin in diameter). As a baseline optical design we have chosen, for now, the CCAT Ritchey-Chretien optical system, with a Cassegrain focal ratio of  $f/8$ , a main reflector focal ratio of  $f/0.6$  and a back focal distance of  $B = 11.0$  m.

These parameters enable operations at the Nasmyth focus of the telescope, allow a receiver cabin of the appropriate size and the construction of a rigid mechanical structure (and elevation bearings positioning) at an acceptable cost, but require quite a large subreflector ( $\sim 3$ m). This implies a possibly expensive secondary, and also a complex and expensive mechanism for nutating the subreflector at frequencies of  $\sim 1$  Hz.

#### 12.3 Pointing and Tracking

The diffraction limited beam for observations at 200 micron is only  $\sim 2$  arcsec and pointing and tracking a 25 m telescope with  $1/10^{\text{th}}$  beam accuracy is a challenging task. Achieving this goal will require careful attention to all aspects of the mount and drive system. As with most radio telescopes it is anticipated that a pointing model will be developed that allows blind (i.e., absolute) pointing anywhere on the sky that is within one or two beam widths to allow for quick source acquisition and refinement of the pointing using bright sub-millimeter sources. The telescope must then be able to *track* the target source to within about  $1/10^{\text{th}}$  of the beam for an hour or so before correcting the pointing on a nearby strong source. Because of the requirement to observe also during the day, it is

desirable to achieve this pointing and tracking performance without a dedicated special offset (optical/IR) guiding system.

### 13 Extension to Mid-InfraRed

The large aperture and high atmospheric transparency at Dome-C offer unique scientific opportunities for high spatial resolution imaging in the MIR ( $< \sim 40$  micron). The system wavefront error budget of 12 micron rms will not support diffraction limited imaging short of  $\sim 200$  micron with the full aperture of the telescope. On the individual panel scale, however, the wavefront error is significantly diminished.

Alternative options could be: (i) a Fizeau beam combination of many subapertures (panels) spread over the disk would enable inteferometric image reconstruction with the full resolution of a 25m telescope over a narrow field of view (as proposed for CCAT). (ii) Using the first (or first and second) ring(s) of panels of the primary reflector would enable the use of the telescope as a MIR single-dish with the equivalent collecting aperture of a 6.8 m (10.8 m) telescope. Either option would require the panels (assumed here to be 1.84 m, square-like panels) to have IR quality surface and an overall RMS of less than 5 micron. Option (ii) would additionally require the first/second rings of panels to be kept aligned to within MIR specs.

Working document - version 1.0 - CMC/ING meeting